SPIE Conference on Sensor Fusion and Decentralized Control in Autonomous Robotic Systems, Pittsburgh, October 14-17, 1997.

Explaining Finite State Machine Characteristics using Variable Structure Control

John T. Feddema, Rush D. Robinett, Brian J. Driessen*

Sandia National Laboratories
P.O. Box 5800, MS 1003
Albuquerque, NM 87185

ABSTRACT

This paper describes how variable structure control can be used to describe the overall behavior of multiple autonomous robotic vehicles with simple finite state machine rules. The importance of this result is that we can then begin to design provably asymptotically stable group behaviors from a set of simple control laws and appropriate switching points with variable structure control. The ability to prove convergence to a goal is especially important for applications such as locating military targets or land mines.

Keywords: finite state machine, cooperative behavior, robotics, variable structure control, sliding mode control

INTRODUCTION

Probably the most widely used philosophy for control of multiple autonomous vehicles is Rodney Brook's Subsumption architecture [1]. It consists of a layered control system implemented as an augmented finite state machine. After reading sensor inputs, multiple functions are evaluated and a decision is made as to which control law to enforce. The advantage of this architecture is that is fast and simple to implement. The disadvantage is that there is no theory regarding what the control laws should be and when to switch between them. This paper attempts to address some of these issues.

A Variable Structure Control (VSC) system changes the structure (or dynamics) of the system by switching at precisely defined states to another member of a set of possible continuous functions of the state [2-4]. This technique provides the framework to define the appropriate control laws and the switching structure. Lyapunov's direct method is often used to design control surfaces which guide the system to a given goal.

The next section discusses how VSC has been used to analyze the behavior of a single vehicle tracking a line. The following section expands this analysis to multiple vehicles which are to converge to the origin while not running into each other. The last section discusses the conclusions of this work and future research directions.

LINE TRACKING WITH A SINGLE VEHICLE

Sandia National Laboratories (SNL) has recently developed a 16 cm^3 (1 in^3) Miniature Autonomous Robot Vehicle (MARV) which is capable of tracking a single conducting wire carrying a 96kHz signal (see Figure 1). Particular attention was paid to the design of the control system to search out the wire, track it, and recover if the wire was lost.

Approximately 250 lines of assembly code were written to control the vehicle. A set of if/then statements in the embedded software switches between four finite states: SEARCH, ROTATE, TRACK, and BACKUP. Changing from one state to another depends on the current state the program is in and two capacitive sensor measurements. In the state transition diagram in Figure 2, s_l and s_r are the left and right sensor measurements, T_1 and T_2 are

* This work performed at Sandia National Laboratories supported by the U.S. Department of Energy under contract DE-AC04-94AL85000.

constant sensor thresholds, t is the state time, and T_{out} is a constant time-out period. Based on the state decision, the program jumps to different routines which determine the duration of the PWM signals that control the velocities of the two motors. During these routines, the state and time in that state are updated, and each routine ends by going back and reading the sensor inputs. This organization resembles an augmented finite state machine. Similar to the work by Brooks [1], there is a time out associated with each state; however, we do not compute the results of each state in parallel and then decide which state to apply.

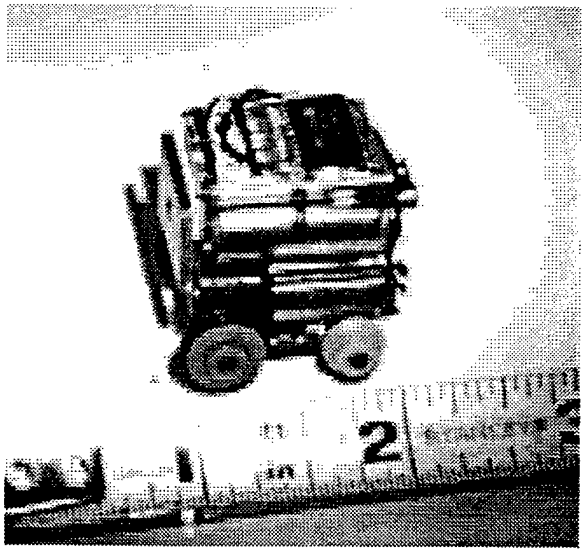

Figure 1. Picture of MARV.

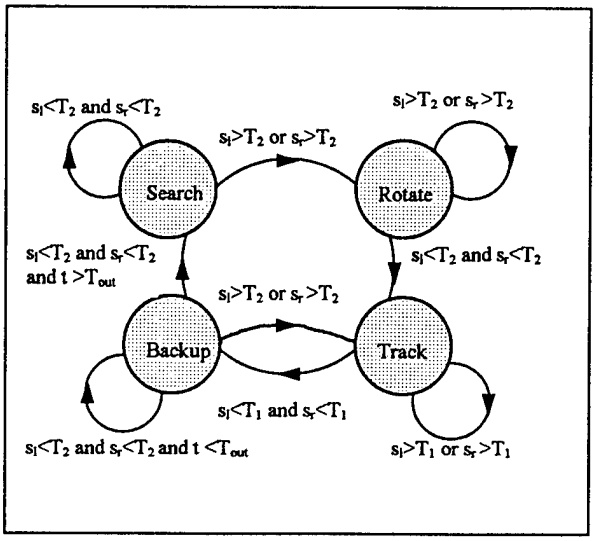

Figure 2. State Transition diagram of MARV.

Both simulations and actual experiments were performed to test the performance of MARV's control. The vehicle tracked the wire as desired, but an interesting phenomenon occurred when approaching the wire at a more perpendicular angle. The vehicle would overshoot when in the TRACK state and then switch into the BACKUP state. By switching between these two states the vehicle was eventually able to track the wire as shown in Figure 3.

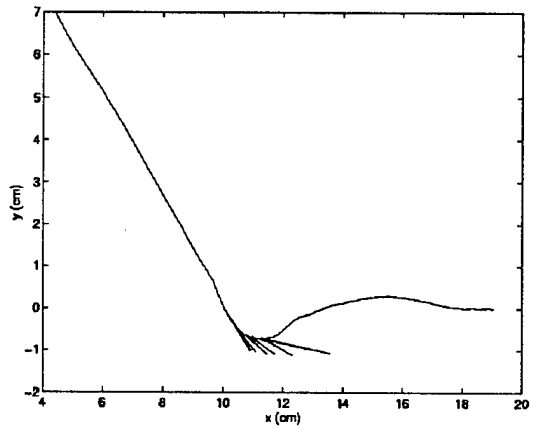

Figure 3. Path of MARV when approached at a 52 degree angle.

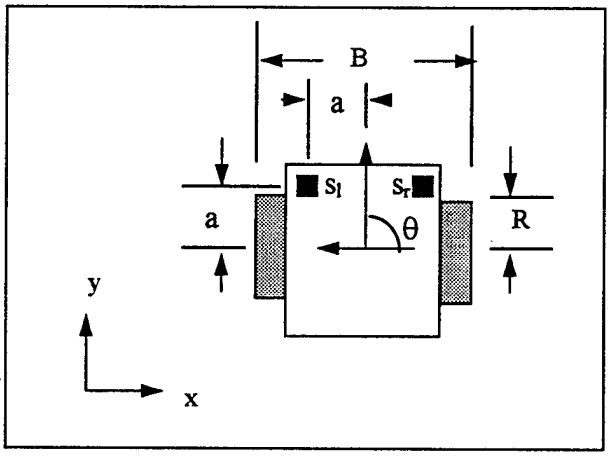

Figure 4. Skid driven vehicle notation.

This behavior might be what some would call emergent. Emergent behavior is generally thought of as a complex behavior arising from the interaction of simple local rules. The simple rules in this case are the control laws in the

DISCLAIMER

TRACK and BACKUP states. The complex behavior is the ability to track the wire at larger angles than the system was initially designed to accommodate.

While emergence is usually viewed as having beneficial properties, it is very difficult to design for in general since it is presently not well understood. Some form of mathematically modeling is needed to explain the phenomenon, and in this paper, VSC is suggested as a means of explaining emergent behavior resulting from finite state machine programming.

Before a VSC can be derived, a model of the system is required. The following is a brief summary of the derivation of the equations of motion of MARV. The derivation is similar to [5] except that the parameters of the right and left sides are assumed equal and the motor's armature effects are added. Referring to Figure 4, the vehicle's equations of motion are

$$M\frac{dv}{dt} = f_r + f_l \tag{1}$$

$$J\frac{d\omega}{dt} = \frac{B}{2}\left(f_r - f_l\right) \tag{2}$$

where B is the wheel base, M is the mass, J is the rotational moment of inertia, and f_r and f_l are forces generated by the right and left wheels. Assuming no slippage, the linear and angular velocities of the vehicle are

$$v = \frac{1}{2}\left(R\omega_r + R\omega_l\right) \tag{3}$$

$$\omega = \frac{1}{B}\left(R\omega_r - R\omega_l\right) \tag{4}$$

where R is the wheel radius, and ω_r and ω_l are the right and left wheel angular velocities. The force generated by each wheel is related to the motor torque, which in turn is related to the applied voltage of the motor by the following equations.

$$\tau_r = \gamma J_m\dot{\omega}_r + \frac{1}{\gamma}\left(J_w\dot{\omega}_r + D\omega_r + R f_r\right) \tag{5}$$

$$\tau_l = \gamma J_m\dot{\omega}_l + \frac{1}{\gamma}\left(J_w\dot{\omega}_l + D\omega_l + R f_l\right) \tag{6}$$

$$\tau_r = \frac{K_I}{\Omega}V_r - \frac{\gamma K_b K_I}{\Omega}\omega_r \tag{7}$$

$$\tau_l = \frac{K_I}{\Omega}V_l - \frac{\gamma K_b K_I}{\Omega}\omega_l \tag{8}$$

where τ_r and τ_l are the right and left motor torque values, γ is the ratio of the motor gearbox, J_m is the moment of inertia about the motor axis, J_w is the moment of inertia about the wheel, D is the friction constant of the wheel, Ω is the motor armature resistance, K_b is the motor's back EMF, K_I is the torque constant, and V_r and V_l are the right and left motor voltages.

The velocity and acceleration of the vehicle in the x and y directions are given by

$$\begin{bmatrix}\dot{x}\\ \dot{y}\end{bmatrix} = v\begin{bmatrix}\cos\theta\\ \sin\theta\end{bmatrix} \tag{9}$$

$$\begin{bmatrix}\ddot{x}\\ \ddot{y}\end{bmatrix} = \dot{v}\begin{bmatrix}\cos\theta\\ \sin\theta\end{bmatrix} + v\dot{\theta}\begin{bmatrix}-\sin\theta\\ \cos\theta\end{bmatrix} \tag{10}$$

Note that $\omega = \dot{\theta}$ and $v = \sqrt{\dot{x}^2 + \dot{y}^2}$. Combining the above equations, the resulting equations of motion are

$$\begin{bmatrix}\ddot{x}\\ \ddot{y}\end{bmatrix}=\begin{bmatrix}\cos\theta\\ \sin\theta\end{bmatrix}\left\{\frac{\gamma K_I}{R\Omega M_{eff}}\left(V_r+V_l\right)-\frac{2}{R^2 M_{eff}}\left(D+\frac{\gamma^2 K_b K_I}{\Omega}\right)\sqrt{\dot{x}^2+\dot{y}^2}\right\}+\begin{bmatrix}-\sin\theta\\ \cos\theta\end{bmatrix}\dot{\theta}\sqrt{\dot{x}^2+\dot{y}^2} \tag{11}$$

and

$$\ddot{\theta}=\frac{\gamma BK_I}{2R\Omega J_{eff}}\left(V_r-V_l\right)-\frac{B^2}{2R^2 J_{eff}}\left(D+\frac{\gamma^2 K_b K_I}{\Omega}\right)\dot{\theta} \tag{12}$$

where the effective mass and moment of inertia are given by

$$M_{eff}=M+\frac{2}{R^2}\left(\gamma^2 J_m+J_w\right) \tag{13}$$

$$J_{eff}=J+\frac{B^2}{2R^2}\left(\gamma^2 J_m+J_w\right) \tag{14}$$

The capacitance sensors are located in front of the vehicle's skid center (see Figure 4) and their positions are given by

$$\left(x_{sr},y_{sr}\right)=\left(x+a\cos\theta+a\sin\theta,\,y+a\cos\theta-a\sin\theta\right) \tag{15}$$

$$\left(x_{sl},y_{sl}\right)=\left(x+a\cos\theta-a\sin\theta,\,y+a\cos\theta+a\sin\theta\right) \tag{16}$$

The output voltage of the sensors (s_r and s_l) is inversely proportional to the distance from the wire. If we assume that the vehicle is tracking a straight wire along the x axis, then the sensor measurements are given by

$$s_r=1\Big/\sqrt{\left(y+a\cos\theta-a\sin\theta\right)^2+h^2} \tag{17}$$

$$s_l=1\Big/\sqrt{\left(y+a\cos\theta+a\sin\theta\right)^2+h^2} \tag{18}$$

where h is the height of the sensor from the wire. During the TRACK state, the proportional control law with gain G is:

$$\text{If } s_r\geq s_l\text{, then } V_r=V_o \text{ and } V_l=V_o+G\left(s_r-s_l\right). \tag{19}$$

$$\text{If } s_r<s_l\text{, then } V_r=V_o+G\left(s_l-s_r\right) \text{ and } V_l=V_o. \tag{20}$$

The constant voltage V_o keeps the vehicle moving forward. During the BACKUP state, both the left and the right voltages are $-V_o$.

By switching between the TRACK and BACKUP states when the sensor values reach predefined thresholds, the motion of the vehicle follows the trajectory in the phase plane plot in Figure 5. In the SEARCH state, the vehicle approaches the line at a fixed orientation θ. During the TRACK state, the vehicle will asymptotically orient itself over the line and θ will go to zero if θ is small. If θ is too large, the vehicle will overshoot the line and the controller will switch to the BACKUP state. Once the vehicle has backed up over the line, the controller will again switch into the TRACK state. This is repeated until θ is small enough to converge to the origin.

This phase plot can be more easily interpreted if we linearize the sensor model and substitute into Equation (12). Assuming that the sensor is straddling the wire and that $y=0$ and $h=0$, the control law may be reduced to

$$\text{If } s_r\geq s_l\text{, then } V_r-V_l=-\frac{2G\sin\theta}{a\cos 2\theta}. \tag{21}$$

$$\text{If } s_r<s_l\text{, then } V_r-V_l=\frac{2G\sin\theta}{a\cos 2\theta}. \tag{22}$$

For small angles of θ , the control law can be approximated as:

$$V_r - V_l = \frac{2G}{a}\theta \tag{23}$$

Substituting into Equation (12), the resulting equation of motion during the tracking state is the familiar second order underdamped system:

$$\ddot{\theta}(t) + 2\xi\omega\dot{\theta}(t) + \omega^2\theta(t) = 0 \tag{24}$$

During the SEARCH and BACKUP states, the control is open loop (i.e., the capacitance sensors are not used). Since $V_r = V_l$, the resulting equation of motion is

$$\ddot{\theta}(t) + \frac{1}{\tau}\dot{\theta}(t) = 0 \tag{25}$$

Therefore, during the TRACK state, the vehicle moves along a trajectory approximately equal to a stable second order response. If this trajectory leads the vehicle outside the range of the sensors, a threshold value is reached and the controller goes into the BACKUP state. The BACKUP state moves the vehicle in a vertical line in the phase plane plot of θ. Another threshold is reached when the vehicle straddles the wire, and the controller goes back into the TRACK state. This process is repeated until the vehicle is on a trajectory which is within the range of the sensors.

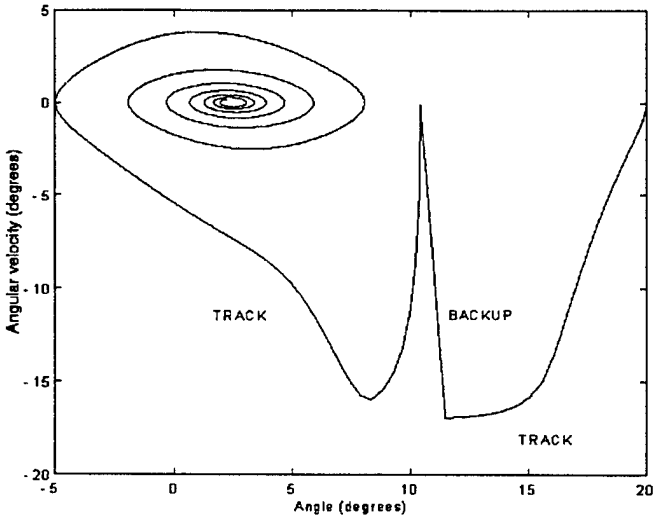

Figure 5. Phase plane trajectory using full nonlinear dynamics and simple MARV control laws. Transitions occur between TRACK, BACKUP, and TRACK states.

This simple example shows how VSC can be used to analyze and design asymptotically convergent finite state machine control laws. The next section will apply VSC to the control of multiple vehicles performing a coordinated motion.

GOAL SEARCHING WITH MULTIPLE VEHICLES

Consider N skid-driven vehicles distributed on a planar surface. The goal of these vehicles is to go towards the origin without running into each other. The N subsystems can be described by the following nonlinear dynamics:

$$\ddot{\mathbf{x}}_i(t) = \mathbf{f}(\mathbf{x}_i(t), \dot{\mathbf{x}}_i(t)) + \mathbf{B}(\mathbf{x}_i(t))\mathbf{u}_i(t) \qquad i = 1, \ldots, N \tag{26}$$

where

$$\mathbf{x}_i(t) = \begin{bmatrix} x_i \\ y_i \\ \theta_i \end{bmatrix} \qquad \text{and} \qquad \mathbf{u}_i(t) = \begin{bmatrix} V_{ri} \\ V_{li} \end{bmatrix}$$

and $\mathbf{f}(\mathbf{x}_i(t), \dot{\mathbf{x}}_i(t)) \in \Re^{3\times 1}$ and $\mathbf{B}(\mathbf{x}_i(t)) \in \Re^{3\times 2}$ are given in Equations (11) and (12). When the vehicles are not close to one another, we can define a sliding surface which is directed to the origin as

$$\mathbf{s}_i(t) = \mathbf{W}_i\mathbf{x}_i + \widetilde{\mathbf{W}}_i\dot{\mathbf{x}}_i = 0 \text{ where } \mathbf{W}_i = \begin{bmatrix} w_{1i} & 0 & 0 \\ 0 & w_{2i} & 0 \end{bmatrix} \text{ and } \widetilde{\mathbf{W}}_i = \begin{bmatrix} \widetilde{w}_{1i} & 0 & 0 \\ 0 & \widetilde{w}_{2i} & 0 \end{bmatrix} \tag{27}$$

The nonzero diagonal terms can be used to prescript the transient response while on the sliding surface. The equivalent control is determined by setting the time derivative of the sliding surface to zero and solving for the control.

$$\dot{\mathbf{s}}_i(t) = \mathbf{W}_i\dot{\mathbf{x}}_i + \widetilde{\mathbf{W}}_i\ddot{\mathbf{x}}_i = \mathbf{W}_i\dot{\mathbf{x}}_i + \widetilde{\mathbf{W}}_i\mathbf{f}\left(\mathbf{x}_i, \dot{\mathbf{x}}_i\right) + \widetilde{\mathbf{W}}_i\mathbf{B}(\mathbf{x}_i)\mathbf{u}_i = 0 \tag{28}$$

Therefore, the equivalent control on the sliding surface is given by

$$\mathbf{u}_i = \left[\widetilde{\mathbf{W}}_i\mathbf{B}(\mathbf{x}_i)\right]^{-1}\left[-\mathbf{W}_i\dot{\mathbf{x}}_i - \widetilde{\mathbf{W}}_i\mathbf{f}\left(\mathbf{x}_i, \dot{\mathbf{x}}_i\right)\right] \tag{29}$$

When not on the sliding surface (in the reaching mode), the term $-\mathbf{A}_i\,\mathrm{sgn}(\mathbf{s}_i)$, where $\mathbf{A}_i$ is positive definite, may be added to drive the system to the sliding surface.

$$\mathbf{u}_i = \left[\widetilde{\mathbf{W}}_i\mathbf{B}(\mathbf{x}_i)\right]^{-1}\left[-\mathbf{W}_i\dot{\mathbf{x}}_i - \widetilde{\mathbf{W}}_i\mathbf{f}\left(\mathbf{x}_i, \dot{\mathbf{x}}_i\right) - \mathbf{A}_i\,\mathrm{sgn}(\mathbf{s}_i)\right] \tag{30}$$

We can prove asymptotic stability of the reaching control with the Lyapunov candidate function

$$V_i = \frac{1}{2}\mathbf{s}_i^T\mathbf{s}_i \geq 0 \tag{31}$$

For an asymptotically stable solution, the time derivative of the Lyapunov function must be less than zero.

$$\dot{V}_i = \mathbf{s}_i^T\dot{\mathbf{s}}_i = -\mathbf{s}_i^T\mathbf{A}_i\,\mathrm{sgn}(\mathbf{s}_i) < 0 \tag{32}$$

As seen in the equations above, the control is valid only if the inverse of $\widetilde{\mathbf{W}}_i\mathbf{B}(\mathbf{x}_i)$ exists. Unfortunately, $\widetilde{\mathbf{W}}_i\mathbf{B}(\mathbf{x}_i)$ is singular for Equation (11). This difficulty occurs because we are trying to control three free variables, $\mathbf{x}_i$, with only two control parameters, $\mathbf{u}_i$. If the state vector is modified to drive a point p in front of the vehicle to the origin, the number of free variables is reduced to two. If the distance to p is a in the moving body frame, then

$$\begin{aligned} x_p &= x + a\cos\theta \\ y_p &= y + a\sin\theta \\ \dot{x}_p &= \dot{x} - \dot{\theta}a\sin\theta \\ \dot{y}_p &= \dot{y} + \dot{\theta}a\cos\theta \end{aligned} \tag{33}$$

$$\ddot{x}_p = \ddot{x} - \dot{\theta}^2 a\cos\theta - \ddot{\theta} a\sin\theta$$

$$\ddot{y}_p = \ddot{y} - \dot{\theta}^2 a\sin\theta + \ddot{\theta} a\cos\theta$$

The state equations can be rewritten as

$$\ddot{\mathbf{p}}_i(t) = \tilde{\mathbf{f}}(\mathbf{p}_i(t), \dot{\mathbf{p}}_i(t)) + \tilde{\mathbf{B}}(\mathbf{p}_i(t))\mathbf{u}_i(t) \tag{34}$$

where

$$\mathbf{p}_i(t) = \begin{bmatrix} x_{pi} \\ y_{pi} \\ \theta_i \end{bmatrix}$$

$$\tilde{\mathbf{f}}(\mathbf{p}_i, \dot{\mathbf{p}}_i) = \begin{bmatrix} -\left(K_1 v_i + a\dot{\theta}_i^2\right)\cos\theta_i + \left(aK_2 - v_i\right)\dot{\theta}_i \sin\theta_i \\ -\left(K_1 v_i + a\dot{\theta}_i^2\right)\sin\theta_i + \left(-aK_2 + v_i\right)\dot{\theta}_i \cos\theta_i \\ -K_2\dot{\theta}_i \end{bmatrix}$$

$$\tilde{\mathbf{B}}(\mathbf{p}_i) = \begin{bmatrix} K_3\cos\theta_i - aK_4\sin\theta_i & K_3\cos\theta_i + aK_4\sin\theta_i \\ K_3\sin\theta_i + aK_4\cos\theta_i & K_3\sin\theta_i - aK_4\cos\theta_i \\ K_4 & -K_4 \end{bmatrix}$$

$$v_i = \sqrt{\dot{x}_{pi}^2 + \dot{y}_{pi}^2 + a^2\dot{\theta}_i^2 + 2a\dot{\theta}\left(\dot{x}_{pi}\sin\theta_i - \dot{y}_{pi}\cos\theta_i\right)}$$

$$K_1 = \frac{2}{R^2 M_{eff}}\left(D + \frac{\gamma^2 K_b K_I}{\Omega}\right) \qquad K_2 = \frac{B^2}{2R^2 J_{eff}}\left(D + \frac{\gamma^2 K_b K_I}{\Omega}\right)$$

$$K_3 = \frac{\gamma K_I}{R\Omega M_{eff}} \qquad K_4 = \frac{\gamma B K_I}{2R\Omega J_{eff}}$$

Since $\tilde{\mathbf{W}}_i\tilde{\mathbf{B}}(\mathbf{p}_i)$ is not singular, and the sliding mode control in Equation (30) (with $\mathbf{p}_i$, $\tilde{\mathbf{f}}(\mathbf{p}_i, \dot{\mathbf{p}}_i)$, $\tilde{\mathbf{W}}_i\tilde{\mathbf{B}}(\mathbf{p}_i)$ replacing $\mathbf{x}_i$, $\mathbf{f}(\mathbf{x}_i, \dot{\mathbf{x}}_i)$, and $\tilde{\mathbf{W}}_i\mathbf{B}(\mathbf{x}_i)$) can be used to guide the vehicles to the origin. However, multiple vehicles will run into each other since there is no feedback between them which would drive them apart.

Fortunately, recent work on decentralized VSC (or DVSC) of interconnect systems [6-8] provides some tools for designing a controller which provide vehicle avoidance and at the same time guide them towards the origin. Let the dynamics be defined as:

$$\ddot{\mathbf{p}}_i(t) = \tilde{\mathbf{f}}(\mathbf{p}_i(t), \dot{\mathbf{p}}_i(t)) + \tilde{\mathbf{B}}(\mathbf{p}_i(t))\left[\mathbf{u}_i(t) + \mathbf{g}\left(\mathbf{p}_i(t), \mathbf{p}_j(t)\right)\right] \tag{35}$$

where the term $\mathbf{g}\left(\mathbf{p}_i(t), \mathbf{p}_j(t)\right)$ is the interaction between vehicles i and j. A repulsive force, which is proportional to the inverse of the squared distance between the vehicles and directed away from vehicle j, is created when

$$\mathbf{g}\left(\mathbf{p}_i(t), \mathbf{p}_j(t)\right) = K\left(\frac{1}{d^2} - \frac{1}{d_o^2}\right)\left[\tilde{\mathbf{W}}_i\tilde{\mathbf{B}}(\mathbf{p}_i(t))\right]^{-1}\begin{bmatrix} \left(x_{pi} - x_{pj}\right)/d \\ \left(y_{pi} - y_{pj}\right)/d \end{bmatrix} \quad \text{for} \quad d < d_o \tag{36}$$

where K is user specified gain, d is the distance between vehicle i and j, and d_o is a user specified distance within which the repulsive force takes affect. A complementary sliding surface is

$$\mathbf{s}_i(t) = \mathbf{W}_i\mathbf{x}_i + \tilde{\mathbf{W}}_i\dot{\mathbf{x}}_i - \tilde{\mathbf{W}}_i\int_{-\infty}^{t}\tilde{\mathbf{B}}(\mathbf{p}_i)\,\mathbf{g}\left(\mathbf{p}_i(q), \mathbf{p}_j(q)\right)dq \tag{37}$$

The equivalent control is the same as before (Equation 30), and it can be shown that the control is asymptotically stable (i.e. $\dot{V}_i = \mathbf{s}_i^T \dot{\mathbf{s}}_i < 0$).

The response of three vehicles with and without repulsive forces is shown in Figures 6 and 7. In Figure 6, the vehicles move along a diagonal line to the x axis because sliding surface parameters $\mathbf{W}_i$ and $\tilde{\mathbf{W}}_i$ where set equal to the identity matrix. Notice the vehicle run over each other while moving to the origin. In Figure 7, they move along the same sliding surface defined by Equation (29) until they come within d_o of each other. At that point, they switch to the controller with the repulsive force term $\mathbf{g}\left(\mathbf{p}_i(t), \mathbf{p}_j(t)\right)$ and are attracted to the sliding surface defined by Equation (37). The result is that the vehicles swarm about the origin and do not run into each other.

Other behaviors could be added by changing the sliding surface. For example, if the vehicles have only a limited sensing range to the target, an attractive force could be added to attract vehicles which cannot sense the target to those that can.

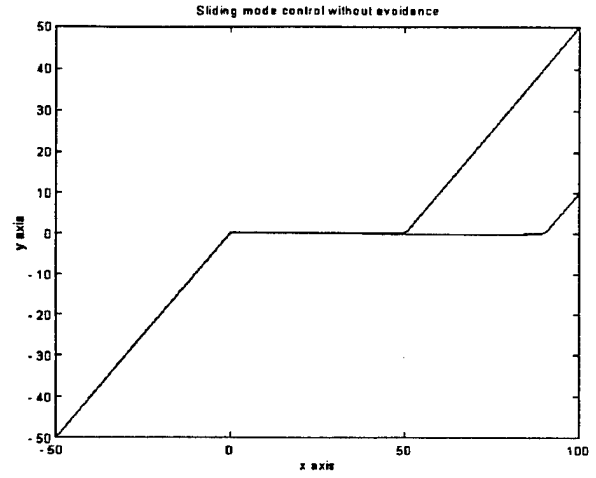

Figure 6. Simulation of 3 vehicles using a sliding mode controller without repulsive forces.

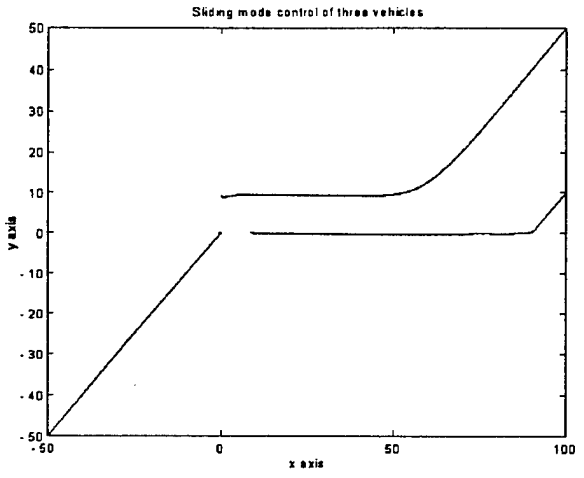

Figure 7. Simulation of 3 vehicles using a sliding controller with repulsive forces to avoid each other.

CONCLUSION

Both the single and multiple vehicle examples show how VSC can be used to analyze and design convergent control behaviors. The single vehicle example showed that switching between finite states can be viewed as the switching of trajectories in the phase plane. For a convergent behavior, it is important to switch onto a trajectory which asymptotically leads to the goal. The multiple vehicle example showed how cooperative motion can be designed using sliding modes. Complex nonlinear problems can be solved by designing several sliding surfaces which perform different tasks and then defining when to switch to the appropriate sliding surface.

ACKNOWLEDGMENTS

The authors greatly appreciate the help of Tom Weber and Barry Spletzer in designing and building MARV.

REFERENCES

[1] R.A. Brooks, "A Robust Layered Control System for a Mobile Robot," *IEEE Journal of Robotics and Automation*, RA-2, pp. 14-23, April 1986.

[2] V.I. Utkin, "Variable Structure Systems with Sliding Modes," *IEEE Transactions on Automatic Control*, Vol. AC-22, No. 2, April 1977.

[3] DeCarlo, R.A, Zak, S.H., Matthews, G.P., "Variable Structure Control of Nonlinear Multivariable Systems," *Proceedings of the IEEE*, Vol. 76, No. 3, March 1988.

[4] V.I. Utkin, *Sliding Modes in Control Optimization*, Springer-Verlag, 1981.

[5] K. Kimoto, S. Yuta, "Autonomous Mobile Robot Simulator - A Programming Tool for Sensor-Based Behavior," *Autonomous Robots*, 1, p. 131-148, 1995.

[6] G.P. Matthews, R.A. DeCarlo, "Decentralized Tracking for a Class of Interconnected Nonlinear Systems Using Variable Structure Control," *Automatic*a, Vol. 24, No. 2, pp. 187-193, 1988.

[7] S. Richter, S. Lefebvre, R. DeCarlo, "Control of a Class of Nonlinear Systems by Decentralized Control," *IEEE Trans. On Automatic Control*, Vol. AC-27, No. 2, April 1982.

[8] Y.V. Orlov, V.I. Utkin, "Use of Sliding Modes in Distributed System Control Problems," *Automation Remote Control*, Vol. 43, No. 9, pp. 1143-1148, 1982.

Report Number (14) SAND--97-2534C
CONF-971086--

Publ. Date (11) 199710
Sponsor Code (18) DOE/MA, XF
UC Category (19) UC-900, DOE/ER

DOE